Bull. Mater. Sci. (2018) 41:51
https://doi.org/10.1007/s12034-018-1571-9

Effect of oxygen vacancies on Li-storage of anatase TiO_2 (001) facets: a first principles study

H CHEN, Y H DING*, X Q TANG, W ZHANG, J R YIN, P ZHANG and Y JIANG
Institute of Rheology Mechanics, Xiangtan University, Hunan 411105, People's Republic of China
*Author for correspondence (yhding@xtu.edu.cn)

MS received 24 June 2017; accepted 17 August 2017; published online 29 March 2018

Abstract. Effect of oxygen vacancies on Li-storage of anatase TiO_2 (001) facets was stimulated by density functional theory (DFT). The lattice parameters, adsorbed energy and energy barriers of TiO_2 with oxygen vacancies were calculated. High adsorption energy of 5.91 eV for Li atoms indicates that oxygen vacancies have a positive effect on the Li storage of nanostructured anatase TiO_2. The theoretical capacity was enhanced by an extra Li atom storaged at the oxygen vacancies.

Keywords. Anatase TiO_2; oxygen vacancies; adsorbed energy; Li storage; DFT.

1. Introduction

As a fascinating material, TiO_2 in anatase phase was widely used as a conventional photocatalyst due to its low cost, high chemical stability, abundance and nontoxicity, especially, its high photoelectric conversion efficiency [1–4]. Nowadays, the applications of TiO_2 extend into various areas of photocatalysis, water-splitting, lithium-ion batteries (LIBs) and solar cells [5–12]. There are three main types of TiO_2 crystal structures, i.e., rutile, anatase and brookite. The application of TiO_2-based materials is mainly dependent on their crystalline structure, morphology, size and exposed facets [13–15]. The conventional understanding of the surface structure of TiO_2 is that facets with a higher percentage of under-coordinated atoms are usually more reactive in heterogeneous reactions. Chen *et al* [16] investigated the photocatalytic reactivity of a set of anatase crystals with predominant {101} or {010} facets [17]. The {010} facets showed the highest photocatalytic reactivity in generating OH radicals and hydrogen evolution. However, synthesis of TiO_2 with exposed high-energy facets is a well-known challenge in many fields of science and technology. Many researchers have attempted to prepare facet-exposed TiO_2 by chemical routes. Until now, several methods were developed to prepare facet-exposed TiO_2, such as hydrothermal synthesis [18], self-transformation strategy [19], solid state reaction [20] and gas-phase oxidation route [21].

Facet-exposed TiO_2 has open tunnel structure and low energy Li^+ pathways from surface to subsurface sites [22]. Those features made facet-exposed TiO_2 as a promising candidate for the anode material in LIBs [23–26]. It was found that Li-ion insertion was favoured on the {001} surface of anatase, as evidenced by a higher charge transfer rate and chemical diffusion coefficient [27]. The maximum capacity of lithium insertion in anatase TiO_2 is 335 mAh g^{-1} (Li_1TiO_2), which can be reached at ultra-small TiO_2 crystal (<7 nm) [28]. As a poor Li-ion conductor, the full occupation of the octahedral voids limits the Li^+ transport in TiO_2 crystal. Recently, Li-storage of MoO_{3-x} with oxygen vacancies was studied by Kim *et al* [29]. The introduction of oxygen vacancies leads to a larger interlayer spacing that promotes faster charge storage kinetics and enables the MoO_3 structure to be retained during the Li^+ insertion/removal. In the same way, it was reported that oxygen vacancies in TiO_2 nanocrystals will favour the Li storage [18,30–33]. Although the experimental evidences supporting the positive effect of oxygen vacancies on the Li storage in oxygen-deficient TiO_2, the mechanism behind this phenomenon is remained unblocked.

In this paper, we studied the Li-storage in the nanostructured anatase TiO_2 (001) surfaces with oxygen vacancies. The effect of oxygen vacancies on the Li-storage of TiO_2 was evaluated by density functional theory (DFT). The lattice parameters, adsorbed energy and energy barriers of TiO_2 with oxygen vacancies were calculated.

2. Computational details

All simulations were carried out using the plane wave pseudopotential method within DFT, as implemented in the CASTEP module. All calculations were performed within the generalized gradient approximation (GGA) [34] and parameterized by the Perdew–Burke–Ernzerhof (PBE) formula [35] for the electron exchange correlation energy. The calculated value is relative and we used the same calculation protocols. TiO_2 (001) surface was simulated using a slab model, which contains five atomic layers in 1×1 super cell, containing 8 O and 4 Ti atoms. The cut-off energy for the plane wave was set

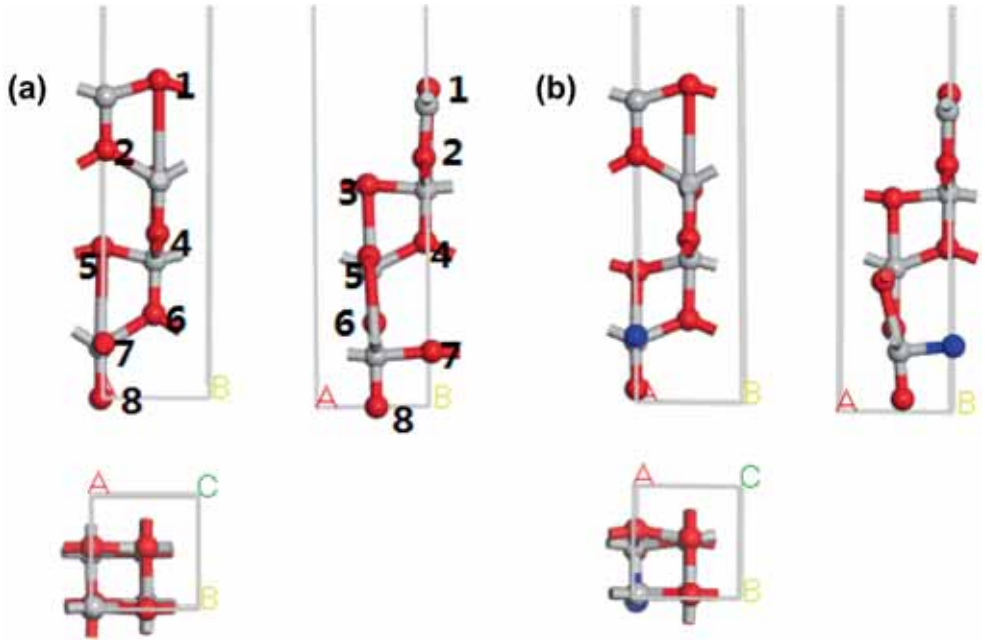

Figure 1. Top and side views of the optimized structure of nanostructured anatase TiO_2 (001) surfaces. (**a**) Without oxygen vacancies and (**b**) with 7-oxygen vacancies. Red sphere represents O atom. Blue sphere represents oxygen vacancy. Numbers 1–8 represent oxygen vacancy sites.

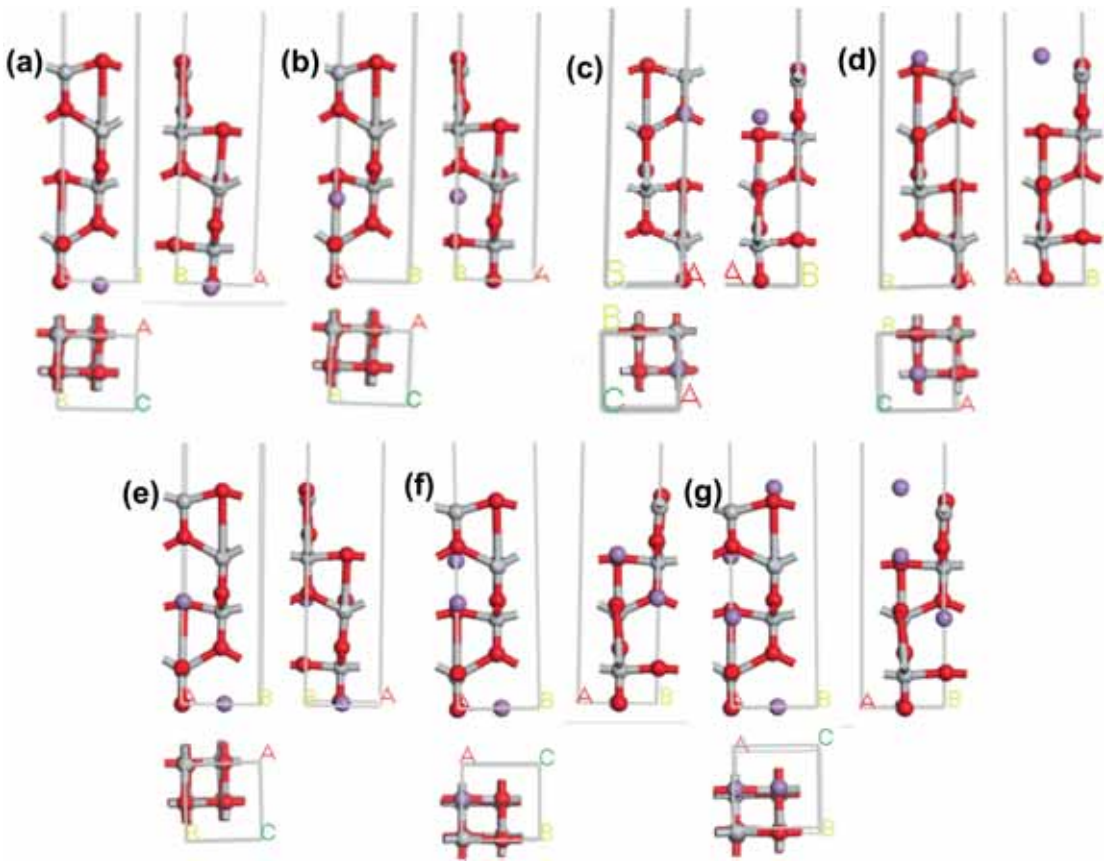

Figure 2. (**a**–**d**) Top and side views of the optimum structure of anatase TiO_2 (001) surfaces adsorbing a single Li atom. (**e**–**g**) Top and side views of the optimum structure of anatase adsorbing 2, 3 and 4 Li atoms.

to 400 eV. The SCF tolerance was 5.0×10^{-6} eV per atom and the convergent tolerance was 5.0×10^{-6} eV per atom. The Brillouin zone of anatase TiO_2 (001) surface was sampled on a $5 \times 5 \times 1$ Monkhorst–Pack grid. Periodic boundary conditions were applied in all directions. A 20 Å vacuum layer was used to avoid unwanted interaction along the sheet thickness. To compute the Li diffusion profiles, we used the LST/QST and NEB tools. The cut-off energy for the plane wave was set to 370 eV. The SCF tolerance was 2.0×10^{-5} eV per atom. The RMS convergent and energy convergence tolerance were 0.05 eV $Å^{-1}$ and 5.0×10^{-5} eV per atom, respectively. The Brillouin zone was sampled on a $5 \times 5 \times 1$ Monkhorst–Pack grid. The binding energy of Li atoms on TiO_2 (001) surface was obtained from:

$$E_b = -\left(E_{TiO2+Li} - E_{TiO2} - n\mu_{Li}\right)/n,$$

where $E_{TiO2+Li}$ is the total energy of the TiO_2 after binding with Li, E_{TiO2} and μ_{Li} are the total energy of TiO_2 and the chemical potential of Li, respectively. n is the number of Li atoms adsorbed in TiO_2 sheet. The computed bulk lattice parameters $a = b = 3.7767$ Å and $c = 9.5990$ Å, in good agreement with reported experimental values $a = b = 3.7848$ Å and $c = 9.5124$ Å [36]. These results indicated that our calculation methods are reasonable.

3. Results and discussion

The top and side views of the optimized structure of nanostructured anatase TiO_2(001) surfaces are shown in figure 1. The optimized lattice parameters are $a = 3.63$ Å, b = 3.75 Å, $c = 11.12$ Å, $\alpha = 90.12°$, $\beta = 89.94°$, $\gamma = 89.99°$, which are consistent with experiments and previous theoretical calculation results. The stability and Li storage of (001) surfaces with oxygen vacancies were simulated. The position of oxygen vacancies is vital to the structural stability and Li insertion of TiO_2. With 2-, 3-, 4-, 5- and 6-oxygen vacancies, the lattice parameters varied greatly and the crystal structure tended to be unstable. Instead, with 1-, 7- and 8-oxygen vacancies, the (001) surfaces underwent slight deformation. Combination of the Li storage and structural stability, anatase TiO_2 (001) surfaces with 7-oxygen vacancies are more favourable to serve as anode materials for LIBs.

Binding energy is another important parameter of anode materials for Li storage. To calculate the binding energy, we simulated the adsorption behaviours of anatase TiO_2 (001) surfaces adsorbed with Li atoms in diverse sites (figure 2). Figure 2a–d display the optimum structure of anatase TiO_2 (001) surfaces adsorbing a single Li atom at four different sites. From figure 2a to d, the binding energy decreases in

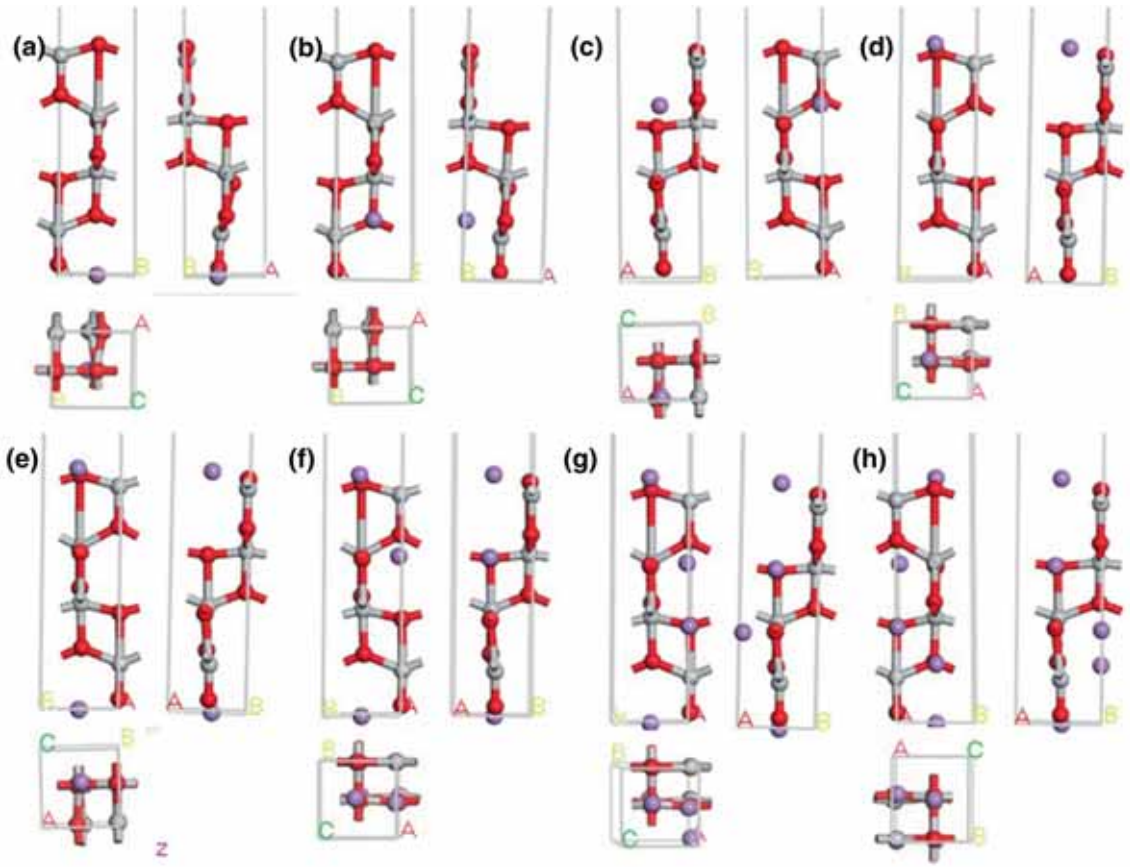

Figure 3. (**a–d**) Top and side views of the optimum structure of anatase TiO_2 (001) surfaces with oxygen vacancies adsorbing a single Li atom. (**e–h**) Top and side views of the optimum structure of anatase adsorbing 2, 3, 4 and 5 Li atoms.

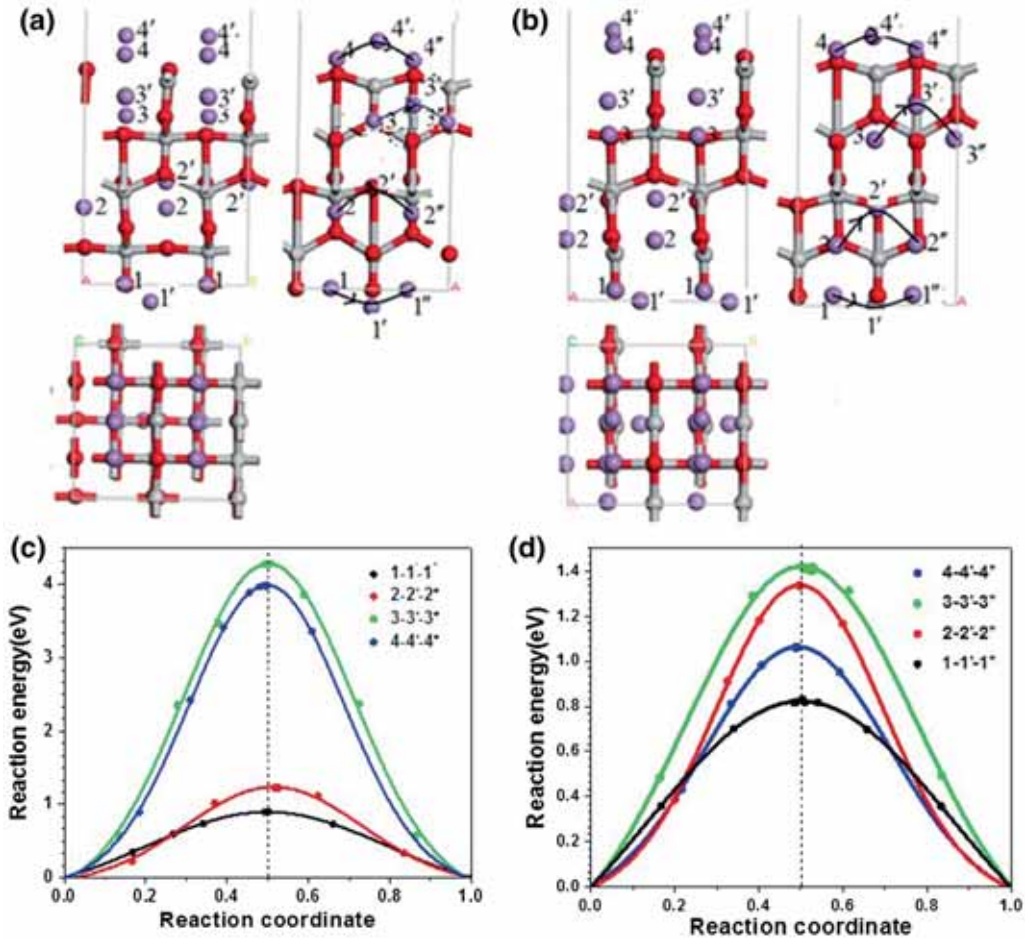

Figure 4. (**a** and **b**) Top and side views of Li diffusion in (001) surfaces without or with oxygen vacancies. (**c** and **d**) Energy profiles of Li diffusion along 1-1′-1″ (2-2′-2″, 3-3′-3″, 4-4′-4″) pathways of Li diffusion in (001) surfaces without or with oxygen vacancies.

an order of 5.91 > 4.44 > 3.48 > 2.86 eV. As presented in figure 2g, the maximum adsorption quantity of Li in anatase TiO_2 (001) surfaces is four atoms, corresponding to high theoretical capacity of 335 mAh g^{-1}.

The binding energy of anatase TiO_2 (001) surfaces with oxygen vacancies and Li atom in diverse sites was calculated. Figure 3a–d display the optimum structures of anatase TiO_2 (001) surfaces with oxygen vacancies and a single Li atom. The anatase TiO_2 (001) surfaces with oxygen vacancies can storage 4 four Li atoms like raw (001) surfaces. An extra Li atom can be storaged at the site of oxygen vacancies. The maximum adsorption quantity of Li in anatase TiO_2(001) surfaces is 5 atoms ($Li_5Ti_4O_7$), corresponding to an ultra-high theoretical capacity of 441 mAh g^{-1}.

Rate capability is an important requirement for a promising anode material for LIBs. The transportation paths of Li atoms and energy profiles were calculated and are presented in figure 4. For figure 4a, the Li atoms in four different sites migrate to the neighbouring units through four pathways. For example, the energy of barriers through 1-1′-1″ in anatase TiO_2 (001) surface is 0.90 eV. The energy barriers through 1-1′-1″ decreased to 0.83 eV for the model with an oxygen vacancy, resulting in a faster Li transportation [30]. Generally, the barriers energies for Li transportation decreased with introduction of oxygen vacancies into TiO_2 structure [37]. Furthermore, the structure remained constant and stable during the process of Li diffusion.

The calculated lattice parameters, adsorbed energy and energy barriers of (001) surfaces absorbed Li atoms are listed in tables 1 and 2. The *c* is the lattice parameter of TiO_2 in the direction of C, not including the height of the vacuum layer. Without the oxygen vacancies or not, the optimal location for Li adsorption is site 1 with the highest adsorbed energy and the lowest energy barriers. After adsorbed Li atom, the lattice parameters of the units increased slightly. The highest capacity of (001) surfaces is four Li atoms, according to a theoretical capacity of 335 mAh g^{-1}. With oxygen vacancies, both the adsorbed energies and barriers energies decreased at the same site. It indicated that the rate capacity

Table 1. The lattice parameters, adsorbed energy and energy barriers of (001) surfaces absorbed Li atoms at different sites.

	a/*b*/*c*	$\alpha/\beta/\gamma$	Adsorbed energy	Energy barriers
Bulk	3.78/3.78/9.73	90.05/89.95/89.98	—	—
(001) surface	3.63/3.75/11.12	90.12/89.94/89.99	—	—
Site 1	3.63/3.71/11.16	90.00/88.32/90.06	5.91	0.90
Site 2	3.76/3.78/10.12	90.42/88.46/90.01	4.44	1.22
Site 3	3.72/3.81/10.74	90.46/88.21/90.02	3.48	4.29
Site 4	3.76/3.76/10.86	90.33/86.65/90.01	2.86	3.98
2 Li atoms	3.72/3.77/10.22	90.69/89.22/89.32	5.11	—
3 Li atoms	3.82/3.79/9.87	89.94/90.00/90.69	4.03	—
4 Li atoms	4.00/3.89/9.75	89.63/87.88/89.98	3.82	—

Table 2. The lattice parameters, adsorbed energy and energy barriers of (001) surfaces with oxygen vacancies absorbed Li atoms at different sites.

	a/*b*/*c*	$\alpha/\beta/\gamma$	Adsorbed energy	Energy barriers
(001) surface	3.66/3.75/10.57	90.02/88.92/90.00	—	—
Site 1	3.62/3.76/10.98	89.82/88.27/89.94	4.15	0.83
Site 2	3.61/3.93/10.72	89.34/89.14/89.98	2.50	1.33
Site 3	3.68/3.93/10.92	90.06/89.08/90.00	2.58	1.41
Site 4	3.69/3.78/11.00	89.87/90.21/90.01	2.70	1.06
2 Li atoms	3.69/3.78/10.80	89.73/89.93/90.05	3.82	—
3 Li atoms	3.65/3.89/10.88	90.54/89.16/90.17	3.25	—
4 Li atoms	3.68/4.09/10.93	89.48/89.13/90.01	2.91	—
5 Li atoms	3.67/4.08/11.55	89.30/88.59/89.97	2.81	—

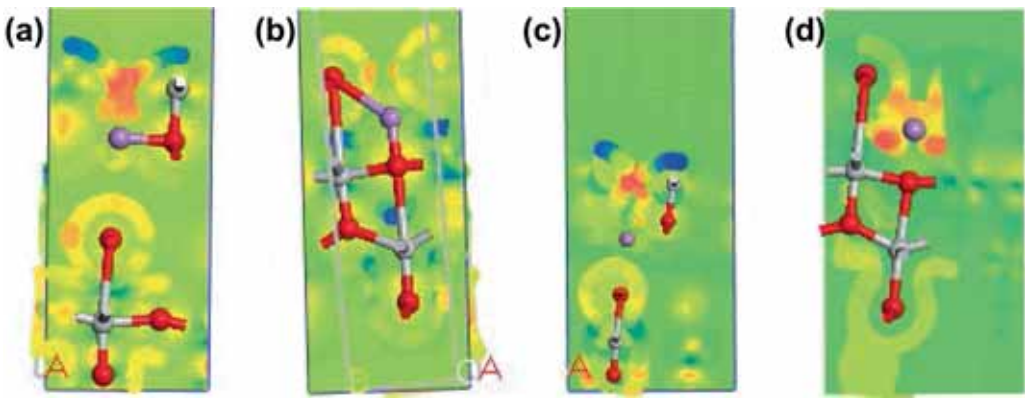

Figure 5. (**a** and **b**) Electron density difference of (001) surfaces at the transition state and initial states. (**c** and **d**) Electron density difference of (001) surfaces with oxygen vacancy at the transition state and initial states.

was improved, but the structural stability was undermined. The oxygen vacancies provide (001) surfaces a higher theoretical capacity in accordance with the previous work [38,39]. The Li–O distances at the transition state and initial states were synthesized. Compared to (001) surfaces without oxygen vacancy, the lower energy barrier for (001) surface with one oxygen vacancy, can be attributed to the differences in the distances and the populations between the Li–O at the transition state and initial states. Figure 5 displays the electron density difference at the transition state and initial states. With one oxygen vacancy at the initial state, the distances (population) of Li ions and the nearby O sites are 1.77 (−0.37), 2.16 (−0.13) and 2.73 (0.02) Å, respectively. At the transition state, the distances are 1.85 (−0.23), 2.53

(−0.03) and 2.58 (−0.24) Å. Without oxygen vacancy, the distance between the Li ions and the nearby O sites are 1.85 (−0.39) and 2.01 (−0.08) Å. At the transition state, the distance between Li ions and the nearby O sites are 1.85 (−0.19), 2.29 (−0.05) and 2.56 (−0.03) Å. For (001) surfaces without oxygen vacancy, from initial to transition state, the number of nearby O atoms interacted with Li ions changed from 2 to 3. For (001) surfaces with oxygen vacancy, the distances between Li ions and nearby O atoms are similar at the transition and initial states. So (001) surfaces without oxygen vacancy have the higher barrier energy than that of (001) surfaces with oxygen vacancy.

4. Conclusions

The effect of oxygen vacancies on the Li storage in (001) surface of nanostructured anatase TiO_2 has been stimulated by first principles DFT. The maximum adsorption quantity of Li in anatase TiO_2(001) surfaces is 5 atoms ($Li_5Ti_4O_7$), corresponding to an ultra-high theoretical capacity of 441 mAh g^{-1}. Lower energy barriers indicates a better rate capability of (001) surface with oxygen vacancies. Our study reveals (001) surface exposed anatase TiO_2 with oxygen vacancies has tremendous potential applications in serving as anode materials for LIBs.

Acknowledgements

The financial support from the National Natural Science Foundation of China (No.21376199 and 51002128), Scientific Research Foundation of Hunan Provincial Education Department (No.17A205 and 15B235), and Postgraduate Innovation Foundation of Hunan Province (No.CX2017B308) is greatly acknowledged.

References

[1] Fujishima A and Honda K 1972 *Nature* **238** 37
[2] Thompson T L and Yates J T 2006 *Chem. Rev.* **106** 4428
[3] Vequizo J J M, Matsunaga H, Ishiku T, Kamimura S, Ohno T and Yamakata A 2017 *ACS Catal.* **7** 2644
[4] Kinya K, Naoya S, Takashi T, Yuichi S, Makoto M, Masaki K *et al* 2016 *Jpn. J. Appl. Phys.* **55** 06GJ08
[5] Cai Y, Wang H E, Zhao X, Huang F, Wang C, Deng Z *et al* 2017 *ACS Appl. Mater. Interf.* **9** 10652
[6] Ding Y H, Zhang P, Ren H M, Zhuo Q, Yang Z M and Jiang Y 2011 *Mater. Res. Bull.* **6** 2403
[7] Qiu B, Xing M and Zhang J 2014 *J. Am. Chem. Soc.* **136** 5852
[8] Ni M, Leung M K H, Leung D Y C and Sumathy K A 2007 *Renew. Sust. Energ. Rev.* **11** 401
[9] Pu Y C, Wang G, Chang K D, Ling Y, Lin Y K, Fitzmorris B C *et al* 2013 *Nano Lett.* **13** 3817
[10] Zeng W, Liu T, Gou Z and Lin L 2012 *Physica E* **44** 1567
[11] Zong Y Z, Zhao S L and Zheng G Z 2010 *J. Phys.: Condens. Matter* **22** 175008
[12] Keisuke N, Takaya K and Yoshinori N 2008 *Appl. Phys. Exp.* **1** 112301
[13] Yu J, Low J, Xiao W, Zhou P and Jaroniec M 2014 *J. Am. Chem. Soc.* **136** 8839
[14] Selcuk S and Selloni A 2016 *Nat. Mater.* **15** 1107
[15] Zhao Z, Tian J, Sang Y, Cabot A and Liu H 2015 *Adv. Mater.* **27** 2557
[16] Chen J S, Tan Y L, Cheah Y and Luan D 2010 *J. Power Sources* **132** 6124
[17] Pan J, Liu G, Lu G Q and Cheng H M 2011 *Angew. Chem. Int. Edit.* **50** 2133
[18] Chen J S, Tan Y L, Li C M, Cheah Y L, Luan D, Madhavi S *et al* 2010 *J. Am. Chem. Soc.* **132** 6124
[19] Liu S, Yu J and Jaroniec M 2010 *J. Am. Chem. Soc.* **132** 11914
[20] Xu H, Reunchan P, Ouyang S, Tong H, Umezawa N, Kako T *et al* 2013 *Chem. Mater.* **25** 405
[21] Jiang H B, Cuan Q, Wen C Z, Xing J, Wu D, Gong X Q *et al* 2011 *Angew. Chem. Int. Edit.* **50** 3764
[22] Dylla A G, Henkelman G and Stevenson K J 2013 *Acc. Chem. Res.* **46** 1104
[23] Cheng X L, Hu M, Huang R and Jiang J 2014 *ACS Appl. Mater. Interf.* **6** 19176
[24] Han H, Song T, Lee E K, Devadoss A, Jeon Y, Ha J *et al* 2012 *ACS Nano* **6** 8308
[25] Chen J S, Archer L A and Wen L X 2011 *J. Mater. Chem.* **21** 9912
[26] Zhou P, Zhu X, Yu J and Xiao W 2013 *ACS Appl. Mater. Interf.* **5** 8165
[27] Hengerer R, Kavan L, Krtil P and Grätzel M 2000 *J. Electrochem. Soc.* **147** 1467
[28] Lafont U, Carta D, Mountjoy G, Chadwick A V and Kelder E M 2009 *J. Phys. Chem. C* **114** 1372
[29] Kim H S, Cook J B, Lin H, Ko J S, Tolbert S H and Ozolins V 2016 *Nat. Mater.* **16** 454
[30] Qiu J L S, Gray E, Liu H, Gu Q F, Sun C, Lai C *et al* 2014 *J. Phys. Chem. C* **118** 8824
[31] Wang W, Lu C H, Ni Y R, Song J B, Su M X and Xu Z Z 2012 *Catal. Commun.* **22** 19
[32] Gordon T R, Cargnello M, Paik T, Mangolini F, Weber R T, Fornasiero P *et al* 2012 *J. Am. Chem. Soc.* **134** 6751
[33] Liu G, Yang H G, Wang X, Cheng L, Pan J and Lu G Q 2009 *J. Am. Chem. Soc.* **131** 12868
[34] Perdew J P, Burke K and Ernzerhof M 1996 *Phys. Rev. Lett.* **77** 3865
[35] Zhang Y and Yang W 1998 *Phys. Rev. Lett.* **80** 890
[36] Burdett J K, Hughbanks T, Miller G J, Richardson J W and Smith J V 1987 *J. Am. Chem. Soc.* **109** 3639
[37] Deng D, Kim M G, Lee J Y and Cho J 2009 *Energy Environ. Sci.* **2** 818
[38] Xia T, Zhang W, Murowchick J B, Liu G and Chen X A 2013 *Adv. Energy Mater.* **3** 1516
[39] Shin J Y, Joo J H, Samuelis D and Maier J 2012 *Chem. Mater.* **24** 543